Detecting Mines in Minefields With Linear Characteristics

Daniel C. I. Walsh

Department of Anthropology
Pennsylvania State University
University Park, PA 16802
(*dcw11@psu.edu*)

Adrian E. Raftery

Department of Statistics
University of Washington
Seattle, WA 98195-4322
(*raftery@stat.washington.edu*)

We consider the problem of detecting minefields using aerial images. A first stage of image processing has reduced the image to a set of points, each one representing a possible mine. Our task is to decide which ones are actual mines. We assume that the minefield consists of approximately parallel rows of mines laid out according to a probability distribution that encourages evenly spaced, linear patterns. The noise points are assumed to be distributed as a Poisson process. We construct a Markov chain Monte Carlo algorithm to estimate the model and obtain posterior probabilities for each point being a mine. The algorithm performs well on several real minefield datasets.

KEY WORDS: Bayesian inference; Classification; Image analysis; Markov chain Monte Carlo; Spatial point process.

1. INTRODUCTION

Detecting minefields, and individual mines, is of interest to civilians and military for purposes of, for example, mine removal in peacetime after the end of conflicts, particularly in countries that have been extensively mined such as Egypt, Cambodia, and Bosnia, or for possible demining in the context of military operations.

Among several ways of detecting mines, one that shows promise is aerial reconnaissance. An aircraft, often unmanned, flies over an area and images it; the images are then analyzed offline or in real time to detect minefields and identify individual mines. This method allows one to survey large areas at relatively low cost and, in particular, at low risk to the personnel involved. One system for doing this is described in the next section.

Critical technical problems arise with this methodology, however. The images produced are often noisy, and mines are hard to identify unambiguously in them. As a result, a first stage of image processing identifies potential mines. This stage often succeeds in identifying many of the mines, but it also tends to identify many other objects as possible mines, such as metal or plastic objects that "look" somewhat like mines to the initial image processing algorithm. The result is a spatial point pattern of possible mine locations. We address in this paper the problem of identifying actual mines in a spatial point pattern containing both mines and clutter.

We distinguish between two related problems. The first is the "field of regard" problem, in which a large area is surveyed aerially, large enough that it can be assumed to contain any minefield in the area (Muise and Smith 1992). Thus the minefield will occupy one part of the image, and the rest of the image will have only clutter and no mines. The analyst's goal is to divide the image into two parts: one with a low intensity spatial point pattern in which only clutter is present, and the other with a higher intensity point process in which both mines and clutter are present. This problem can be solved by assuming that the data are generated by a mixture of two spatial Poisson processes with different intensities and performing statistical inference for this model. Solutions to this problem under different assumptions have been proposed by Allard and Fraley (1997), Byers and Raftery (1997, 1998), Stanford and Raftery (2000), Dasgupta and Raftery (1998), and Fraley and Raftery (1998). The methods proposed worked well, with high detection rates and low false positive rates. Allard and Fraley (1997) provided evidence that the performance of this approach is quite robust to departures from the Poisson assumption.

Here we address the "field of view" problem, in which the area surveyed is much smaller and is likely to be completely or largely contained within the minefield, if a minefield is present. The goal here is to ascertain which of the points reported as mines in the first stage of image processing actually are mines. This is a harder problem, because we cannot use a contrast between intensity levels to solve it. Also, unlike many image analysis problems, it baffles the human eye, which typically cannot pick out mines in such an image. Figure 1 shows one point pattern that we analyzed. The noise level is considerable and the location of the mines is not apparent to the eye.

The minefields of concern here are characterized by nearly parallel, almost linear rows of roughly evenly spaced mines. For several reasons this kind of minefield configuration is common in naval practice and needs to be detected reliably. First, mine-laying forces can remove the mines later more easily, either to facilitate their own operations or to avoid harming civilians, if they have been laid in a regular pattern. A second

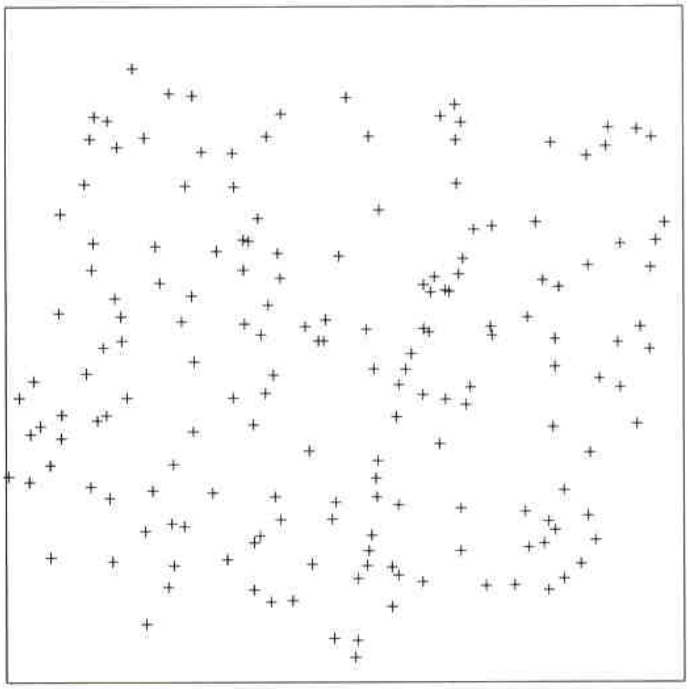

Figure 1. Eglin Air Force Base Minefield Data.

reason is efficient use of assets: The same number of mines can cover a greater area if laid in a regular pattern than in a random or clustered pattern. Third, mines are often laid by machines, which tend to operate in a regular way. Lake and Keenan (1995) summarize why such mine laying procedures are commonly observed:

> From the point of view of military doctrine (e.g., place mines in *nn* rows *xx* meters apart), tactical efficiency (e.g., economic use of resources to ensure coverage against enemy movement), and from inherent limitations in the mine laying process (e.g., safety, inability of humans to emulate a truly random process), it is certainly plausible to hypothesize minefield models which exhibit collinearity, equal spacing, and/or other forms of regularity.

Working at the Naval Coastal Systems Station, Muise and Smith (1995) developed an algorithm for detecting minefields "under the assumption that the minefield has been emplaced such that the mines are laid in a linear pattern, which is a very common mine laying doctrine."

Here we present a method for detecting mines from aerial reconnaissance images in the "field of view" situation. We assume that the images have been preprocessed to produce a collection of points, each one representing the location of a possible mine. Our task is to distinguish between the mines and the false alarms (hereafter referred to as noise or clutter). We develop a flexible model for this type of minefield, namely the sequential placement model. The goal of our approach is to obtain the posterior probability of each point being a mine. We estimate these probabilities and the parameters of the model via Markov chain Monte Carlo in a fully Bayesian framework.

The point pattern from Figure 1 is shown in Figure 2(a) with the mines identified. The results of applying our method to it are shown in Figure 2(b). For these data, the method worked well. The rows of mines were all correctly identified. One false row was detected.

In the next section we describe the datasets we analyzed. In Section 3 we present the sequential placement model. Section 4 outlines the Markov chain Monte Carlo algorithm, and results from applying it to the datasets are presented in Section 5. In Section 6, we discuss the model and possible avenues of future work.

2. COBRA DATA

The Coastal Battlefield Reconnaissance and Analysis (COBRA) program, developed by the U.S. Marine Corps, is intended to detect minefields in coastal areas before troop deployment. An unmanned aerial vehicle, fitted with multispectral video cameras, is flown over the area of interest (see Fig. 3). The video images are either stored or transmitted for processing and analysis. A more detailed description can be found in Witherspoon, Holloway Jr., Davis, Miller, and Dubey (1995).

We base our work on three real datasets, one created by each of the U.S. Air Force, Marine Corps, and Army as representative of at least one kind of situation that they expect to encounter in practice, and brought together and provided to us by the Navy. To create these datasets, landmines were first laid by service personnel in patterns that they viewed as realistic, in the sense of being typical of patterns that might be encountered in peacekeeping or littoral operations, based on actual experience with mines. Then an unmanned aerial vehicle was flown over the area where the mines had been laid. Finally, an initial stage of image processing was applied to obtain a first estimate of possible mine locations. These initially estimated mine locations constitute the raw data for our own work. These data have the advantages of being real and realistic, but with the ground truth known, so that the actual performance of our methods can be assessed on real rather than simulated data.

Eglin Air Force Base and Camp Lejeune

A COBRA image database was obtained from the Navy's Coastal Systems Station, Dahlgren Division, Panama City, Florida. Raw images, ground truth, and the results of their own image processing method were available for two different sites, Eglin Air Force Base, Florida and Marine Corps Base, Camp Lejeune, North Carolina.

The test site at Eglin AFB was contained in an environment cluttered with clumps of grass and patches of sand. One COBRA image from there is shown in Figure 4; the full dataset shown in Figure 1 was obtained by combining 10 overlapping images of this type. The imaged area is approximately 30 meters across. The test site at Lejeune was a moderately cluttered coastal area (see Fig. 5).

The image processing technique used (described in Holmes, Schwartz, Seldin, Wright, and Witter 1995) searched for local anomalies in the multiband images based on a measure of spectral–spatial contrast. This algorithm had been applied to the database, and the top 25 targets for each image were identified. At each site there were 10 overlapping images available. We aligned the images by eye in order to obtain the relative horizontal and vertical displacements of neighboring images. We then concatenated the top 25 targets from each image into a spatial point pattern on a common scale. Given the typical distance between targets, duplicates (targets that were detected

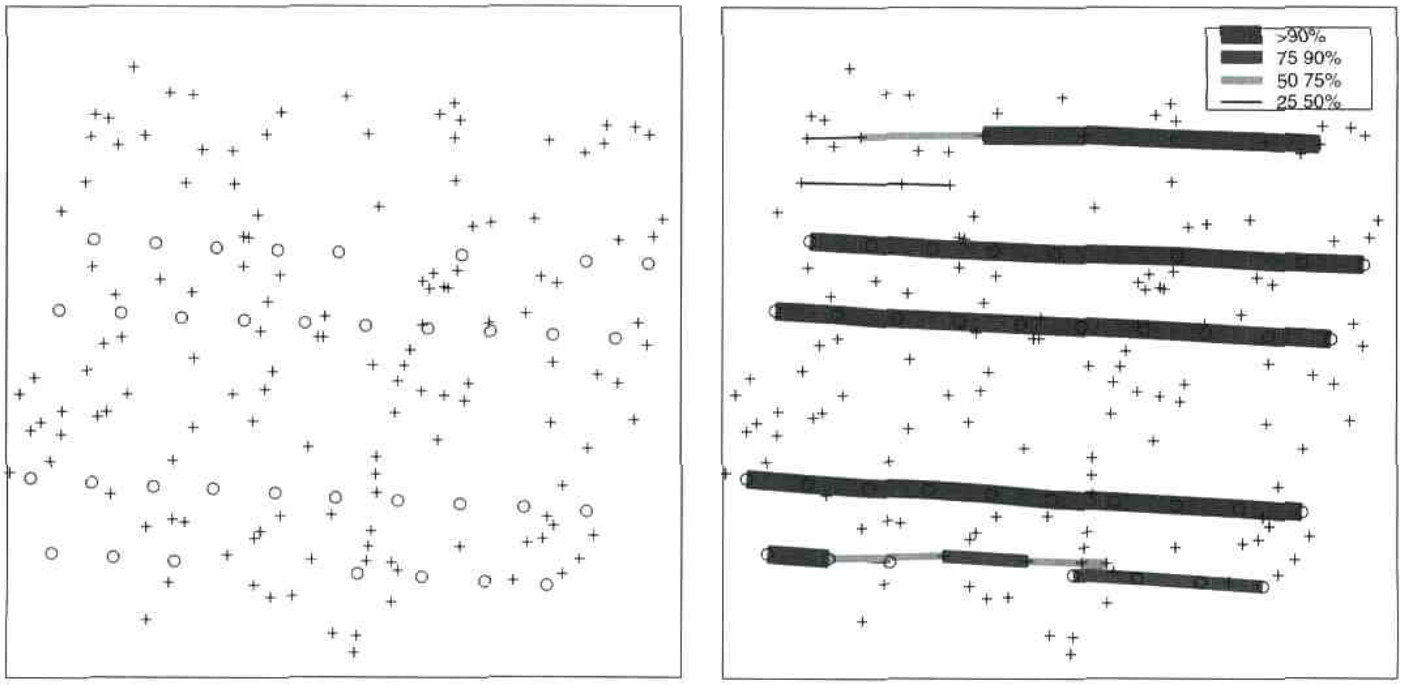

Figure 2. MCMC Results—Eglin Air Force Base. (a) Force base data—mines shown (o = mines, + = noise). (b) Edge classification—Eglin Air Force Base. The widths of the edges are proportional to their posterior probabilities.

in multiple images) were easy to identify and were removed. In the Eglin AFB dataset shown in Figure 2(a), the image processing identified 173 points, of which 35 are mines and 138 are noise points. In the Lejeune dataset, shown in Figure 6(a), 168 points were identified, of which 28 were mines and 140 were noise points.

Surf Zone Data

This dataset (Fig. 6(b)) was produced by processing one spectral band from a multispectral camera showing a ground-based scene of mines laid out in a regular pattern on a surf zone (Lake and Keenan 1995; Lake, Sadler, and Casey 1997). The processed image contained 50 points, which they considered to be clutter-free (i.e., all mines). To test their own minefield detection algorithms they added 50 random points. Thus this dataset is partly real and partly synthetic: The mines are real, but the clutter points are synthetic.

3. A MODEL FOR MINE LOCATIONS: THE SEQUENTIAL PLACEMENT MODEL

In this section, we present the sequential placement model for mine locations. The basic idea is that the mines are laid sequentially, roughly a constant distance apart, in approximately parallel rows; earlier we explained why this is a reasonable expectation. The distances between sequential mines, the mean distances between rows, and the direction of the rows are parameters to be inferred.

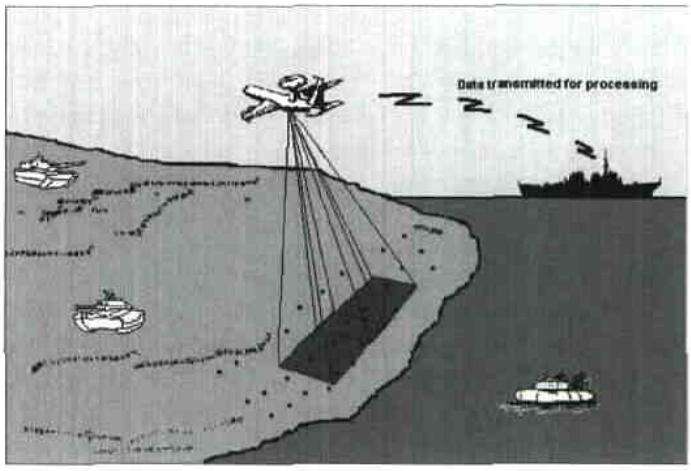

Figure 3. COBRA Operational Concept.

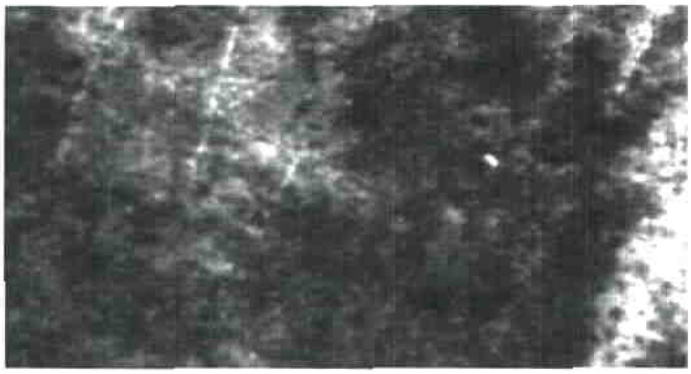

Figure 4. COBRA Image BB081037, Band #1, Right Camera—Eglin Air Force Base.

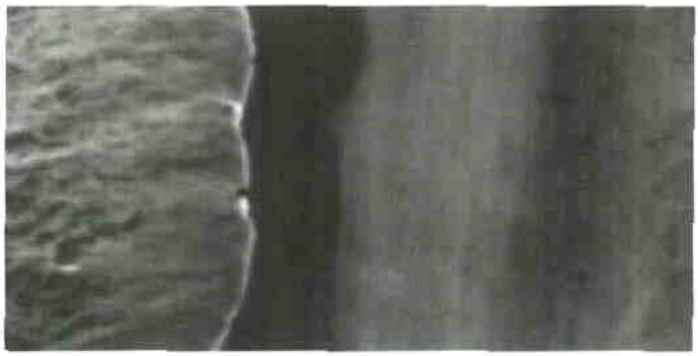

Figure 5. COBRA Image LB560069, Band #1, Left Camera—Camp Lejeune.

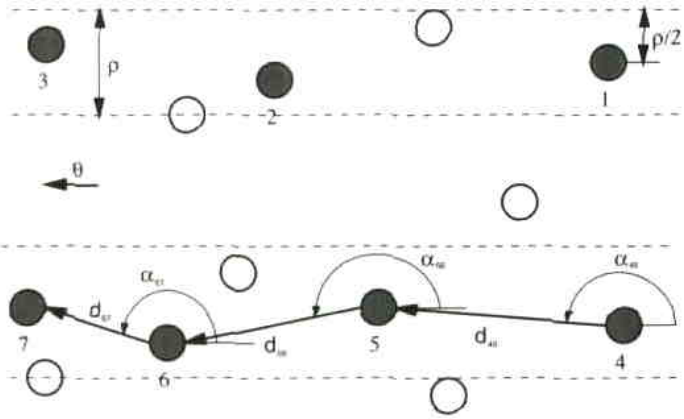

Figure 7. The Sequential Placement Model (• = Mines, ◦ = Noise). Dashed lines represent bands.

3.1 Model Specification

Let A be the sample space or study region, whose area is denoted by $|A|$. Let N be the total number of points, let n_0 be the number of noise points, and let m be the number of mines. The data, i.e., the coordinates of all the points, are denoted by y.

We assume the n_0 noise points are distributed uniformly throughout the study region. This is a simplifying assumption which we have found to work well. It may be, though, that the noise points have their own underlying structure which could be due to, for example, the terrain, trees, or surf. Although possibly more difficult, explicit incorporation of such knowledge could be beneficial.

Suppose that the minefield consists of K rows, and that the ith row contains n_i mines. Thus we have

$$N = n_0 + m = \sum_{i=0}^{K} n_i \quad \text{and} \quad m = \sum_{i=1}^{K} n_i.$$

The mines in each row are ordered and the position of each mine depends on the position of the preceding mine. Let d_{ij} be the Euclidean distance from the ith point to the jth point, and let α_{ij} be the corresponding angle, measured in radians, with horizontal right as a baseline (0 radians). We shall use the notation $i \rightarrow j$ if the ith and jth points are both mines and point j is the next mine after point i in the same row. We assume that, if $i \rightarrow j$, then

$$d_{ij} \sim \text{Normal}(\mu, \sigma^2), \tag{1}$$

$$\alpha_{ij} \sim \text{von Mises}(\theta, \kappa). \tag{2}$$

A schematic of the sequential placement model is shown in Figure 7.

The parameters of the model are described in Table 1 and are denoted by $\Theta = (\mu, \sigma, \theta, \kappa, \rho, \lambda, \nu, \nu_0)$. To prevent rows from overlapping, we add the following constraints. Each row

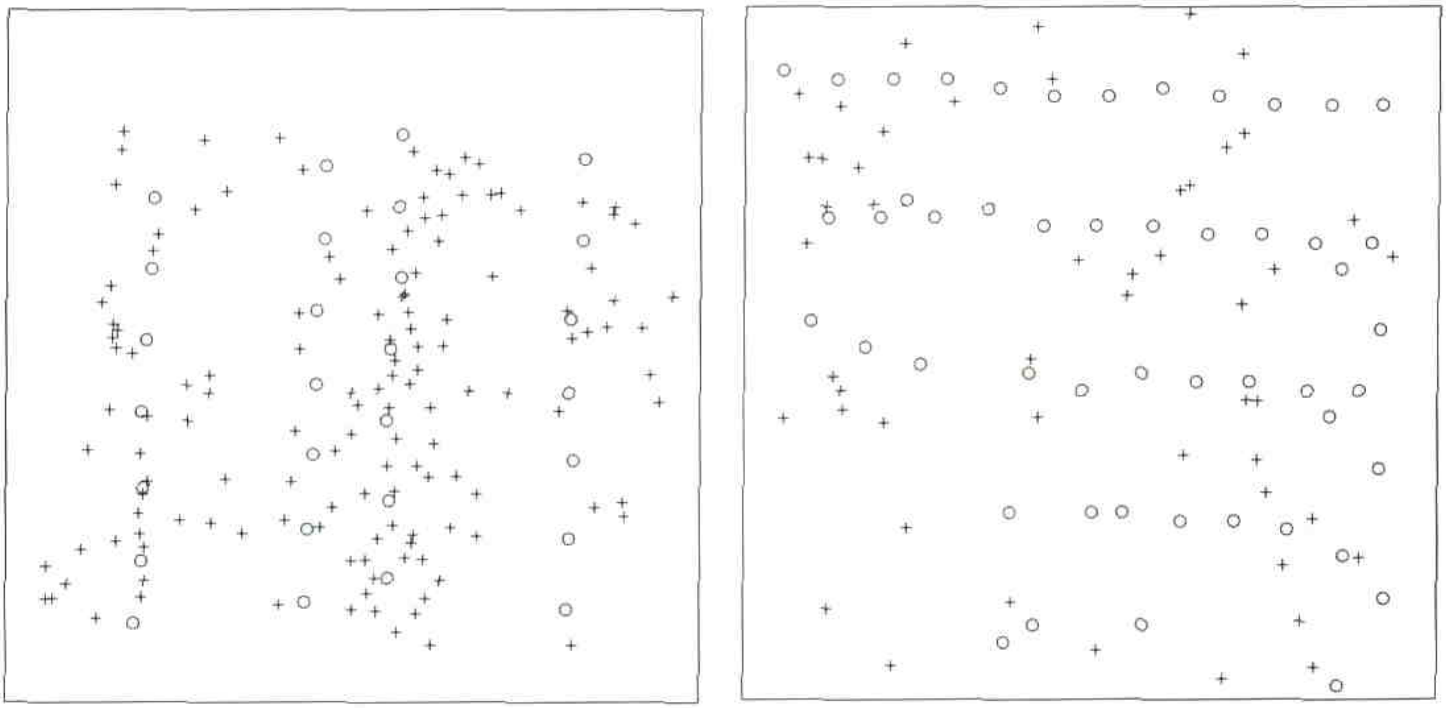

Figure 6. COBRA Datasets. (a) Camp Lejeune data—mines shown (◦ = mines, + = noise). (b) Surf zone data—mines shown (◦ = mines, + = noise).

Table 1. Parameters of the Sequential Placement Model

μ	Mean intermine distance
σ	Standard deviation of intermine distance
θ	Mean intermine distance
κ	Standard deviation of intermine angle
ρ	Row repulsion radius
λ	Mean number of rows
ν	Mean number of noise points per unit area
ν_0	Mean number of mines per line

is assumed to have at least three mines to ensure that the model favors linear features, and each has a "band" of width ρ within which each mine in the row must lie. Each band is centered (perpendicular to θ) on the first mine of each row. Finally, we assume that the first mine in each row is uniformly distributed over the area imaged.

Figure 8 illustrates four possible types of minefield that can be generated with this model, ranging from least to most linear and evenly spaced. The plot shows four rows with 10 mines each. Each row has the same μ and θ, but σ and κ increase from the bottom row to the top row. In the bottom row, both standard deviations are equal to zero, so that all the mines lie on a straight line, and consecutive mines are the same distance apart.

The identities of the mines and their orderings within each row are given by the latent variable, Z, an $N \times N$ matrix, whose individual entries are

$$Z_{ij} = \begin{cases} 1, & \text{if } i \to j, \\ 0, & \text{otherwise.} \end{cases}$$

The variable Z can be thought of as a parameter about which we wish to make inference.

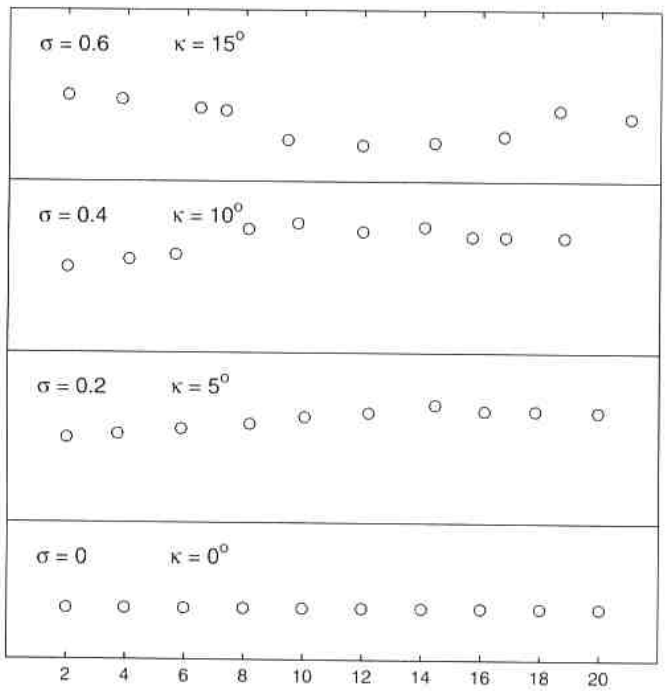

Figure 8. Realizations From the Sequential Placement Model – $\mu = 2$, $\theta = 0°$ (Horizontal right), κ is Converted to Degrees for Convenience.

3.2 Likelihood

The joint probability distribution of the data y and the latent variable Z can be written as

$$P(y, Z \mid \Theta, N, A) = P(y \mid Z, \Theta, N, A)P(Z \mid \Theta, N, A).$$

We condition on the number of points (N) and the area of the study region (A), and assume that at least one row of mines is present.

The likelihood for the data conditional on Z and the model parameters, $P(y \mid Z, \Theta, N, A)$, is given below and is simply a product of the likelihoods of the lengths and the directions of each edge in the minefield, with a term to account for the noise points and a term to ensure that the minefield configuration is allowable. Here Φ_N is the normal (Gaussian) density function, and Φ_{VM} is the von Mises density function:

$$P(y \mid Z, \Theta, N, A) = |A|^{-n_0} \prod_{Z_{ij}=1} \Phi_N(d_{ij} \mid \mu, \sigma) \times \Phi_{VM}(\alpha_{ij} \mid \theta, \kappa) 1(y, Z, \rho),$$

where

$$1(y, Z, \rho) = \begin{cases} 1, & \text{if all mines lie inside the correct,} \\ & \quad \text{bands and no bands overlap,} \\ 0, & \text{otherwise.} \end{cases}$$

Our search for roughly linear structures implies that we expect the standard deviation of the intermine angles to be relatively small. Consequently we parameterized the von Mises distribution in terms of the standard deviation (κ), rather than the usual concentration parameter:

$$\Phi_{VM}(x) = \frac{1}{2\pi I_0(1/\kappa^2)} \exp\left(\frac{1}{\kappa^2}\cos(x-\theta)\right),$$

where $I_0(\cdot)$ is the modified Bessel function of the first kind of order zero. This parameterization made it easier to specify priors that give nonzero density to the lower bound of κ ($\kappa = 0$), which corresponds to a "perfectly laid" minefield. The conditional distribution of Z given Θ, N, and A then factors as follows:

$$\begin{aligned} P(Z \mid \Theta, N, A) &= P(Z \mid \lambda, \nu_0, \nu, N, A) \\ &= P(K, n_0, \ldots, n_K \mid \lambda, \nu, \nu_0, N, A) \\ &= P(n_0, \ldots, n_K \mid K, \nu, \nu_0, N, A)P(K \mid \lambda, N). \end{aligned}$$

This distribution gives the same probability to the Z matrix for all minefields with the same number of rows and the same number of mines per row. $P(n_0, \ldots, n_K \mid \cdot)$ is a multinomial distribution, truncated to ensure that all rows have at least three mines:

$$\begin{aligned} &P(n_0, \ldots, n_K \mid K, \nu, \nu_0, N, A) \\ &\quad \propto \binom{N}{n_0 \cdots n_K} \left(\frac{\nu_0|A|}{\nu_0|A| + K\nu}\right)^{n_0} \\ &\qquad \times \prod_{i=1}^{K} \left(\frac{\nu}{\nu_0|A| + K\nu}\right)^{n_i} 1_{\mathcal{A}}(n_1, \ldots, n_K) \\ &\quad \propto \binom{N}{n_0 \cdots n_K} \frac{\nu^m \nu_0^{n_0} |A|^{n_0}}{(\nu_0|A| + K\nu)^N} 1_{\mathcal{A}}(n_1, \ldots, n_K), \end{aligned}$$

where $\mathcal{A} = \{(n_1, \ldots, n_K) : \min\{n_1, \ldots, n_K\} \geq 3\}$.

The prior on the number of rows is a Poisson distribution, truncated such that the number of rows is at least one and no more than $N/3$, namely

$$P(K \mid \lambda, N) \propto \frac{\lambda^K e^{-\lambda}}{K!} 1_{\mathcal{B}}(K),$$

where $\mathcal{B} = \{K : 1 \le K \le \lfloor \frac{N}{3} \rfloor\}$.

3.3 Simulating From the Sequential Placement Model

A spatial point process is "any stochastic mechanism which generates a countable set of events in the plane" (Diggle 1983). For the sequential placement model to be a valid point process, it must be possible to generate realizations from it. A simple procedure to accomplish this is *rejection sampling*. Using this, a realization from the sequential placement model with parameters Θ can be generated as follows:

1. Sample the number of rows, K, from $P(K \mid \lambda, N)$.
2. Sample the number of noise points, n_0, and the number of mines per row, $n_1, \ldots, n_K$ from $P(n_0, \ldots, n_K \mid K, \nu, \nu_0, N, A)$.
3. Sample K points uniformly from A to denote the locations of the starting mines in each row.
4. For each value i from 1 to K, draw n_i samples from the inter-mine distance and angle distributions (Equations (1) and (2)). Use these distances and the locations of the starting mines to create the locations the mines.
5. Sample n_0 points uniformly from A to denote the locations of the noise points.
6. Concatenate the locations of the mines and the noise points to form the data, y.
7. Calculate the value of the indicator function, $1(y, Z, \rho)$. If this is 1, then stop; else return to step 1.

4. BAYESIAN ESTIMATION VIA MARKOV CHAIN MONTE CARLO

We now describe a fully Bayesian approach to estimate the parameters for the sequential placement model via a Markov chain Monte Carlo (MCMC) algorithm (specifically a Metropolis–Hastings algorithm (Hastings 1970)). See, e.g. Gilks, Richardson, and Spiegelhalter (1996), for an introduction to MCMC methods.

4.1 Priors

The prior distribution is decomposed as follows:

$$\begin{aligned}\pi(\Theta \mid N, A) &= \pi(\mu, \sigma, \theta, \kappa, \rho, \lambda, \nu, \nu_0 \mid N, A) \\ &= \pi(\mu)\pi(\sigma)\pi(\theta)\pi(\kappa)\pi(\rho)\pi(\lambda)\pi(\nu)\pi(\nu_0).\end{aligned}$$

This decomposition is chosen mostly for simplicity, but it also allows us to take account of the prior information that was available to us. For simplicity, we specified all the prior distributions to be uniform. We attempted to create priors for each dataset that might correspond to the knowledge that an expert would have. In particular we assumed that the terrain of the imaged region would provide some prior knowledge about the direction of the minefield. Thus we used priors on θ with width 90° in each case. Note that a totally uninformative prior on θ would have width 180°, since a given minefield would be equally well modeled by θ or $\theta + 180°$. The priors for each dataset were the same (except for θ) and are given in Table 2.

Table 2. Priors Used for the Sequential Placement Model

Parameter	Bounds
μ	(.06, .12)
σ	(.0, .04)
θ (Eglin and surf zone)	(135°, 225°)
θ (Lejeune)	(45°, 135°)
κ	(0, 1.5°)
ρ	(.08, .12)
λ	(2, 4)
ν	(10, 15)
ν_0	(30, 150)

NOTE: All priors are uniform with the bounds shown.

4.2 Proposal Distributions

For the non-negative-valued univariate parameters (σ, κ, ρ, λ, ν, ν_0), a new value was generated by multiplying the current value of the parameter by $\exp(U)$ where $U \sim \text{Normal}(0, \tau^2)$. Note that τ can be different for each parameter and should not be too large, as otherwise no move will be accepted.

For μ a new value was proposed by adding a normal random variable to its current value. We proposed new values for θ by adding a normally distributed random variable to it (modulo 2π).

For the edge matrix Z, six different types of proposals are used: Add, Delete, Swap, Grow, Kill, and Jump. At any given iteration of the MCMC algorithm, either all the univariate parameters are proposed to be updated (individually, in random order), or one of the edge matrix moves is proposed. The different edge proposals are described below and are represented schematically in Figure 9. The first five moves are designed to explore the current mode of the posterior locally. The Jump move is intended to enable the chain to make large jumps from one posterior mode to another. Which type of move is proposed depends on a specified probability vector $p_{\text{Prop}} = (p_{\text{Par}}, p_{\text{Add}}, p_{\text{Delete}}, p_{\text{Swap}}, p_{\text{Grow}}, p_{\text{Kill}}, p_{\text{Jump}})$. For all simulations, $p_{\text{Prop}} = (.15, .15, .15, .15, .15, .15, .10)$.

Add: An end mine (the first or last mine in a row), point i say, is selected at random. A noise point is then proposed to be added to the end (or beginning) of the row. The probability of proposing noise point j (p_{ij}) is proportional to l_{ij}, where l_{ij} is the likelihood of the new edge created by adding the proposed noise point; i.e.,

$$p_{ij} \propto l_{ij} = \Phi_{\text{N}}(d_{ij} \mid \mu, \sigma)\Phi_{\text{VM}}(\alpha_{ij} \mid \theta, \kappa).$$

The proposal probabilities depend on the current parameter values, which increases the mixing of the chain.

Delete: An end mine is chosen at random. Rows with only three mines are ignored. If the move is accepted, the selected end mine is changed to a noise point.

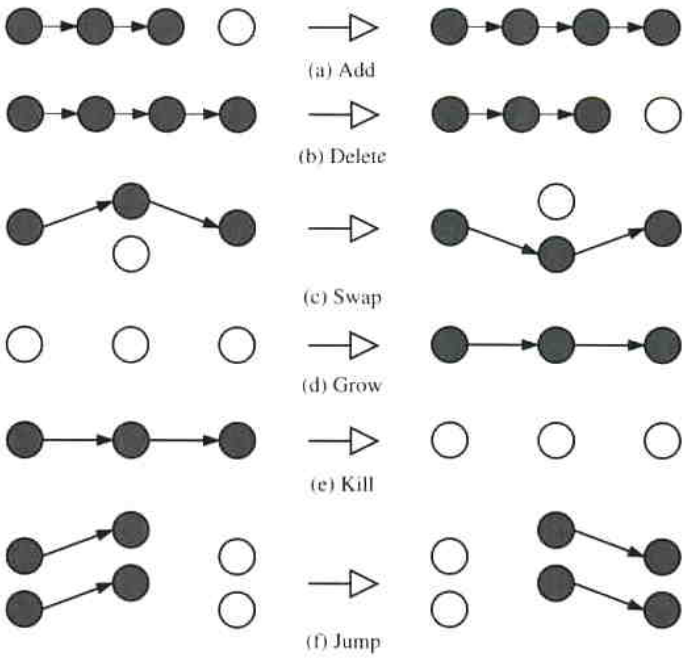

Figure 9. Schematic Representing the Result of Accepting the Different Proposal Moves for Z. Current minefields are shown on the left, and the result of accepting the move is shown on the right. Mines are represented by solid circles while the noise points are represented by open circles. Edges are represented by directed arrows. (a) Add, (b) delete, (c) swap, (d) grow, (e) kill, and (f) jump.

Swap: A mine is chosen at random. A noise point is then proposed to be swapped for this mine. Like **Add**, the probability of proposing a particular noise point is proportional to the likelihood of the new edge(s) that would be created by replacing the proposed noise point and the selected mine.

Grow: A noise point is selected at random; denote its location by (x', y'). The closest two noise points to $(x' - \mu^* \cos\theta^*, y' - \mu^* \sin\theta^*)$ and $(x' + \mu \cos\theta, y' + \mu \sin\theta)$ are then selected, where μ^* and θ^* are the current values of μ and θ, respectively. These three points form are proposed as a new row.

Kill: A row with exactly three mines is selected at random from all rows with exactly three mines, if any. If the move is accepted all three mines in this row will be changed to noise points. This move is not proposed if there is only one row in the minefield.

Jump: The Jump move proposes new model parameters and "grows" a new minefield based on these parameters. This move allows the Markov chain to make large jumps throughout the parameter space. The details of the move can be found in the Appendix.

4.3 MCMC Implementation

The MCMC algorithm was run on the three datasets. In each case, the chain was initialized by drawing the univariate parameters from the priors and creating an initial minefield with a Grow move. Thus the chain started with one row consisting of three mines.

In each case, the chain was run for 1.6 million iterations. This large number was needed due to the slow mixing of the chain. Only every 400th iteration was recorded to reduce storage space. Convergence of the chain to the equilibrium distribution was monitored by running multiple chains from different starting points, which all converged to the same solution. More formally, the Gelman–Rubin R statistic (Gelman and Rubin 1992) was consistent with convergence.

The `gibbsit` software (Raftery and Lewis 1992, 1996) was used to assess the number of iterations needed to estimate the posterior quantiles of interest after reaching the region of high posterior probability and verified the sufficiency of this number of iterations. Note that convergence and adequacy of the number of iterations are different issues. Convergence is achieved once the chain has reached the region of high posterior probability for the first time; estimation accuracy depends on the number of iterations after convergence has been achieved.

5. RESULTS

For each dataset we plotted the posterior probabilities of each edge over the point pattern (Figs. 2(b) and 10, (a) and (b)). It is clear that the method has been quite successful in identifying the rows of mines. In the Eglin AFB dataset, all the rows of mines were identified quite decisively, and most of the false positives produced by the initial image processing were eliminated. For the Camp Lejeune dataset, the rows of mines were correctly identified, and most of the remaining false positives lay close to the actual rows of mines. Operationally, this means that most of the safe areas were correctly identified. In the surf zone dataset, where the mines are less systematically laid out, four of the five rows of mines were still correctly identified. The bottom row of mines, which was far from linearly laid out, was not identified.

Figure 11, (a)–(c), plots the posterior probabilities that each point was a mine for each dataset. The distinction between mines and clutter is clear and accurate for the Eglin AFB dataset. For the Camp Lejeune dataset, almost all the mines had substantial probabilities of being mines, but so did several of the clutter points, because many clutter points were aligned with the main rows of actual mines. For the surf zone dataset, almost all the points with substantial probabilities of being mines actually were, which is good, but quite a few actual mines had low probabilities of being mines. Operationally, this is still useful: A good initial estimate of mine rows and safe areas could be obtained for demining and planning purposes, but care would still need to be taken throughout the area.

These plots are summarized by Receiver Operating Characteristic (ROC) curves in Figure 11(d). The ROC curves are created by plotting the detection rate versus the false alarm rate for many different thresholds of the posterior probabilities that each point is a mine. The ideal curve will be vertical from the origin to (0, 1) and then horizontal. The curve for the Eglin AFB data approximates this ideal rather well, while the results for the noisier Camp Lejeune and surf zone data do not come as close.

Table 3 shows detection and false positive rates from our method. The false positive rate is defined as the empirical conditional probability that a point is declared to be a mine

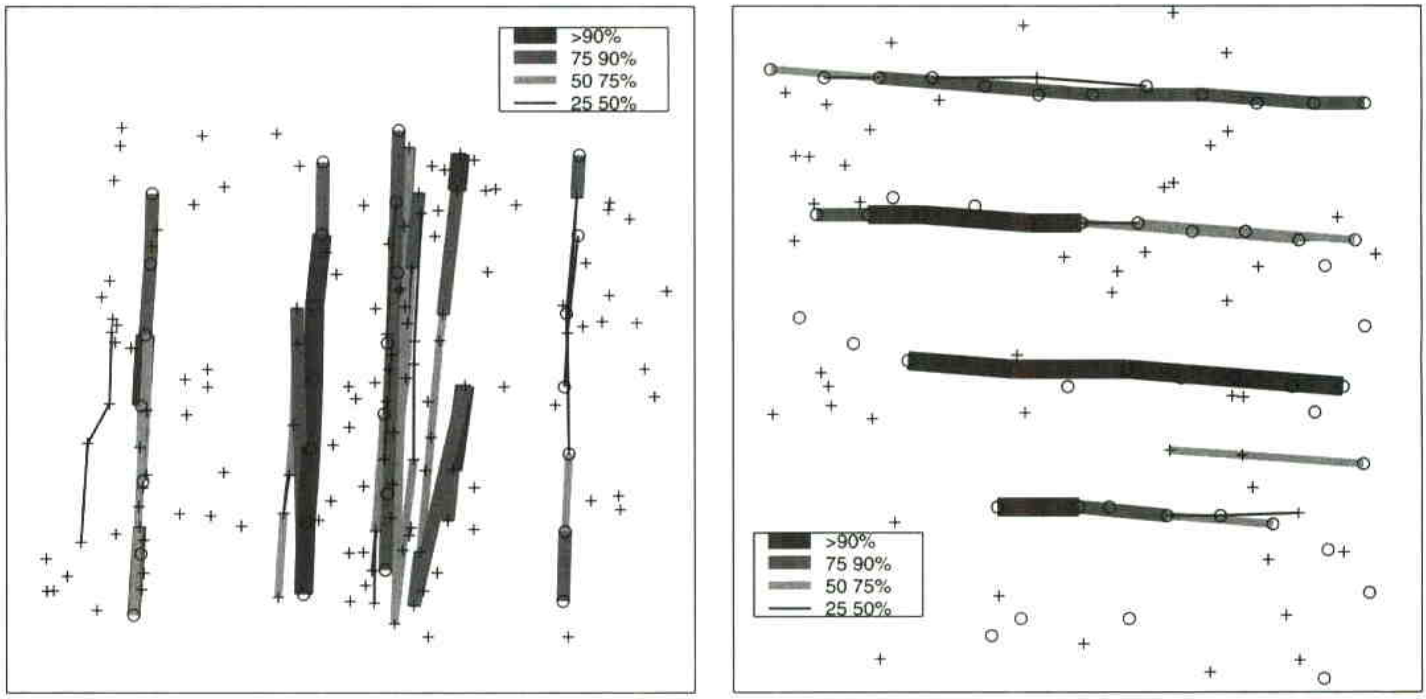

Figure 10. MCMC Results—Camp Lejeune and Surf Zone Datasets. (a) Edge classification—Camp Lejeune. (b) Edge classification—surf zone. The widths of the edges are proportional to their posterior probabilities.

given that it is not one. A conservative 20% probability threshold was chosen for illustrative purposes; the results are relatively insensitive to the precise threshold selected. We considered other thresholds, and 20% does seem to give satisfactory results. For the Eglin AFB data, our method detected all the mines and had a false positive rate of 10%; i.e., it reduced the number of false positives by 90%. Thus it reduced the number of clutter points in the image from 138 to 14, without missing a single mine.

For the Camp Lejeune data, our method also had a 100% detection rate, but a higher false positive rate. This seems to reflect the noisier nature of the data: Many of the false positives were on or close to the actual rows of mines. For the surf zone data, the false positive rate was low, but the detection rate was also disappointingly low, at 66%. Of the 50 mines present, 17 were not detected, including the 6 mines at the bottom of the picture, laid out in a nonlinear pattern. This nonlinearity is the most significant violation of our central assumption in any of the three datasets. The other 11 nondetected mines missed lay for the most part on or very close to the rows of mines that were detected by the algorithm, so their nondetection was less serious in a practical sense.

6. DISCUSSION

We have presented a model for representing the locations of mines in a minefield characterized by nearly parallel rows of roughly equally spaced mines, in the presence of noise. We also outlined a method for fitting this model via Markov chain Monte Carlo. When applied to real data with a substantial amount of noise, the discrimination between the mines and the noise ranged from excellent (Eglin) to moderately good (Lejeune and surf zone), but in each of the three cases the rows of mines were correctly identified, except in the case of one of the five rows of mines in the surf zone dataset. We should note, however, that success here may or may not translate to other datasets and would have to be confirmed by further studies.

MCMC methods are computationally intensive. However, our simulations ran reasonably quickly. For instance the Eglin dataset took about 2,000 CPU seconds for 1.2 million iterations on a DEC Alpha workstation. It may well be possible to reduce the number of iterations without adverse effect. In any event, this time is well within the desired operational specifications. The time required is $O(n)$, where n is the total number of points.

Prior selection is an important issue. Here we have used rather weak or diffuse prior information, but in practice, considerable prior information is often available. For instance, the terrain of the study region will be known and may influence the orientation of the minefield and the spacing of the mines. The results shown here assume that prior information has narrowed the possible orientation angles to a 90° span. This is rather broad, and in practice more precise expert information might well be available which would improve the algorithm's performance.

Here we have focused on the post-image-processing phase of mine detection. Improvements in mine detection results could also be achieved by improving the image processing algorithm itself. The MM-MNF algorithm (Banerji and Goutsias 1995; Braga-Neto and Gousias 1998) has been successfully applied to COBRA images. The false alarm rate in their processed images is lower than in the point patterns we considered, which were obtained with a different and more widely used algorithm. Clutter does remain, however, so there will continue to be a need for methods such as the one we have outlined here.

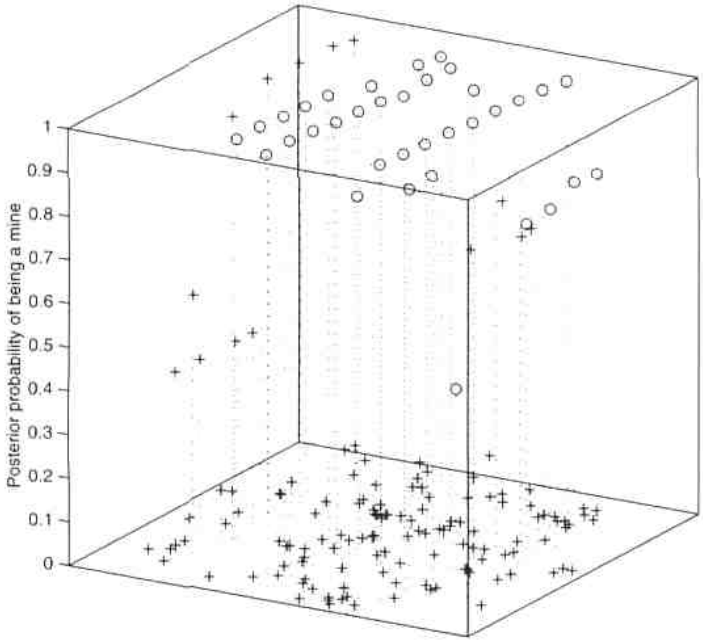

(a) Mine classification - Eglin Air Force Base (o = Mines, + = Noise).

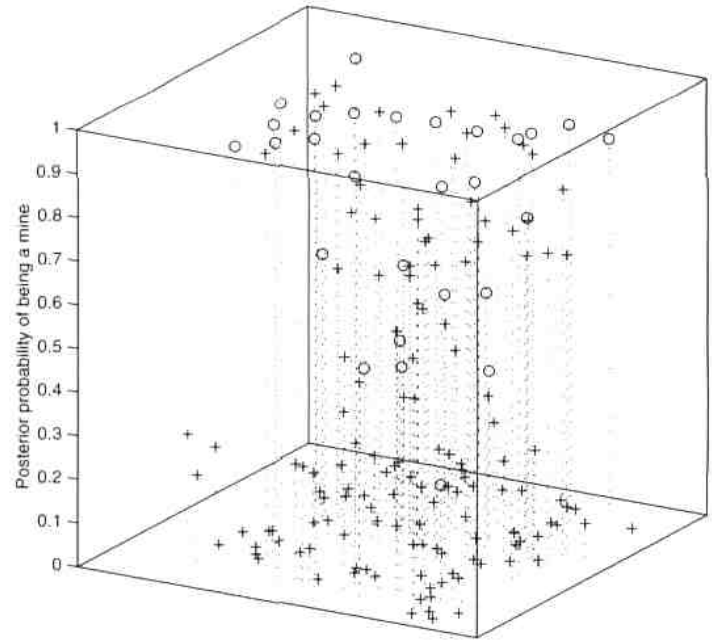

(b) Mine classification - Camp Lejeune (o = Mines, + = Noise).

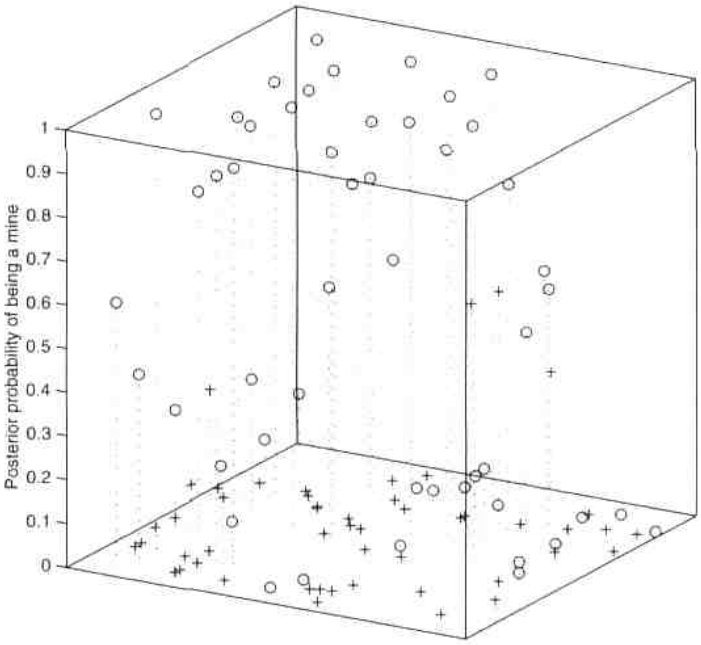

(c) Mine classification - Surf Zone (o = Mines, + = Noise).

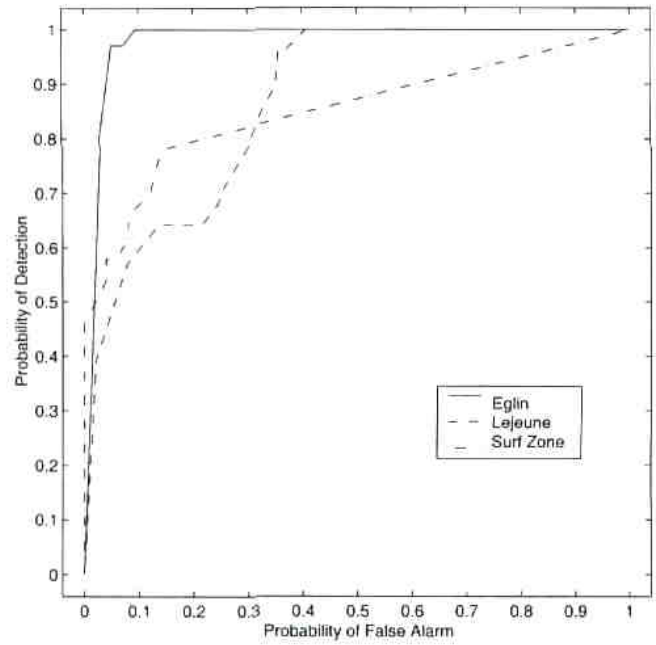

(d) Receiver Operating Characteristic (ROC) curves.

Figure 11. MCMC Results—Mine Classification. (a) Eglin Air Force Base, (b) Camp Lejeune, (c) Surf Zone (o = Mines, + = Noise) and (d) ROC Curves.

Our approach is to model the output of an image processing algorithm as a point process. In doing so, we combine two ideas used in the minefield literature: modeling approximate linearity and regularity of the minefield, and using a Bayesian framework to obtain posterior probabilities of each point being a mine. Cressie and Lawson (2000) also fitted a Bayesian hierarchical point process model via MCMC to a subset of the Camp Lejeune dataset. The linear structure of the minefield was not as obvious in this smaller dataset, but the mines were more regularly spaced than the noise points. Their implementation of the model aimed to detect minefields displaying this local inhibition. Those analyzing this dataset in practice would have had access to the full data that we have used, and so they could have taken advantage of the linear features that underlie our method and whose presence in the data becomes clearer when the full dataset is used.

A different way of detecting approximate linearity and regularity was developed by Lake and Keenan (1995) and Lake et al. (1997). They developed a two-stage algorithm. First, approximately collinear points were identified using a variant of the Hough transform (Hough 1962), and then the spacing of the mines was estimated using a modified Euclidean

Table 3. Detection and False Positive Rates (for a 20% threshold) for Each Dataset

Dataset	Detection rate	False positive rate
Eglin	100	10
Lejeune	100	42
Surf zone	66	8

algorithm. Muise ad Smith (1995) developed an algorithm for minefield detection that also exploits linear patterns. A critical difference between this approach and ours is that ours is based on an explicit statistical model. This leads directly to good estimation methods using established statistical principles and also gives one an idea of when the approach is likely to work well and when it is not. It also suggests ways of improving the method's performance in different situations, by modifying the model so as to exploit background knowledge more effectively.

We have assumed throughout that a minefield is present in the region imaged, and that the analyst's task is to detect the mines. Another important question is to determine whether the region surveyed is part of a minefield or not. A fairly straightforward solution to this problem is available by casting it as one of comparing the minefield model that we have developed with a model for clutter only, such as a homogeneous Poisson process. This can be done by computing the Bayes factor (Kass and Raftery 1995) for one model against the other. There are now several effective ways of computing Bayes factors from MCMC output, e.g., Raftery (1996), DiCiccio, Kass, Raftery, and Wasserman (1997), and references therein.

ACKNOWLEDGMENTS

This research was supported by the Office of Naval Research Grants N00014-96-1-0192 and N00014-96-1-0330. The authors are grateful to Christian Posse for helpful comments.

APPENDIX: JUMP PROPOSAL MOVE DETAILS

The Jump move allows the Markov chain to move large distances in the parameter space in a single iteration. The steps involved in the Jump move are:

1. Propose new univariate parameters.
2. Propose a new number of rows and mines per row (K' and $n'_0, \ldots, n'_{K'}$).
3. Propose new start mines.
4. Grow new rows.

In our simulations for steps 1 and 2 above, we proposed new values only for the minefield orientation parameter θ. The proposed value θ' was drawn from the prior on θ. When proposing new start mines, it is important to ensure that the proposed mines are valid, i.e., that the bands of width ρ centered on the start mines in direction θ do not overlap. A secondary concern is that the calculation of the probability of the proposed mines not be too computationally expensive.

Our approach is to first project all points onto a line perpendicular to θ', and sort each point by its distance *along* this line. Next, associate a *selection probability* p_i to each point. We based p_i on the distance to the projection line. If this distance is small (in the lower quartile of all such distances) we set $p_i = 0.9$; else we set $p_i = 0.1$. This is to encourage starting mines to be near the "front" of the data.

We now select K' mines sequentially from left to right along the projection line. To do this, we first place $K' - 1$ nonoverlapping bands as far to the right as possible while being centered on a point in the direction θ' as in Figure A.1(a). We then select one of the points to the left of the bands (the solid circles in the figure) with probability proportional to p_i. This point is the first start mine. We now move the leftmost band and place it on this point (Fig. A.1(b)). This creates a new set of candidate points from which the next start mine can be selected (Fig. A.1(c)). This procedure is repeated until K' start mines are selected. Once the start mines have been selected, the remaining mines in each row are added sequentially with probability proportional to the likelihood of edge created, as in the Add move.

[Received September 1999. Revised May 2001.]

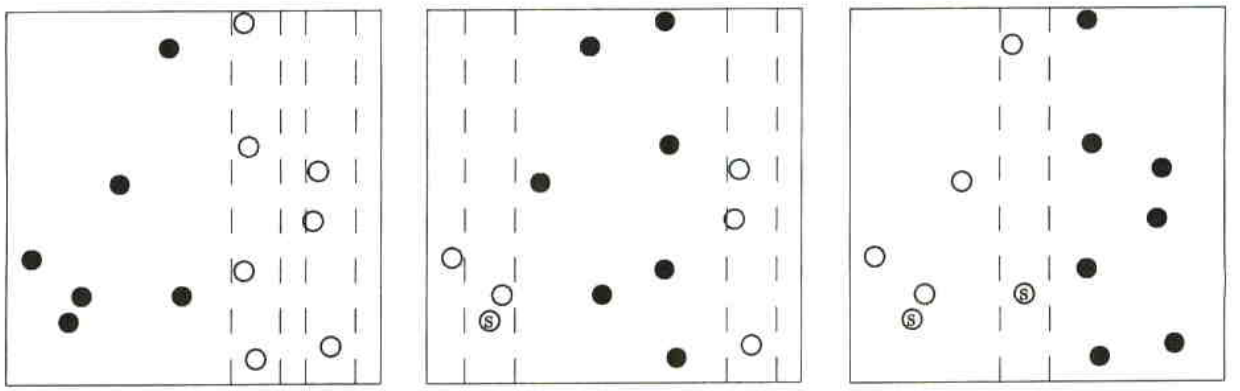

(a) Before selection of the first start mine. (b) First start mine selected. (c) Second start mine selected.

Figure A.1. Selection of the First Two Start Mines: $K' = 3$, • = candidate point, S = start mine. (a) Before selection of the first start mine. (b) First start mine selected. (c) Second start mine selected.

REFERENCES

Allard, D., and Fraley, C. (1997), "Non-parametric Maximum Likelihood Estimation of Features in Spatial Point Processes Using Voronoï Tessellation," *Journal of the American Statistical Association*, 92, 1485–1493.

Banerji, A., and Goutsias, J. (1995), "Detection of Minelike Targets Using Grayscale Morphological Image Reconstruction," in *Detection and Remediation Technologies for Mines and Minelike Targets*, Volume 2496 of *Proceedings of SPIE*, eds. A. C. Dubey, I. Cindrich, J. M. Ralston, and K. Rigano, pp. 836–849.

Braga-Neto, U. M., and Goutsias, J. (1998), "On Detecting Mines and Minelike Objects in Highly Cluttered Multispectral Aerial Images by Means of Mathematical Morphology," in *Detection and Remediation Technologies for Mines and Minelike Targets III*, Volume 3392 of *Proceedings of SPIE*, eds. A. C. Dubey, J. F. Harvey, and J. T. Broach, pp. 987–999.

Byers, S. D., and Raftery, A. E. (1997), "Bayesian Estimation and Segmentation of Spatial Point Processes Using Voronoï Tilings," Technical Report 326, University of Washington, Department of Statistics.

——— (1998), "Nearest Neighbor Clutter Removal for Estimating Features in Spatial Point Processes," *Journal of the American Statistical Association*, 93, 557–584.

Cressie, N., and Lawson, A. B. (2000), "Hierarchical Probability Models and Bayesian Analysis of Mine Locations," *Advances in Applied Probability*, 32, 315–330.

Dasgupta, A., and Raftery, A. E. (1998), "Detecting Features in Spatial Point Processes With Clutter via Model-Based Clustering," *Journal of the American Statistical Association*, 93, 294–302.

DiCiccio, T. J., Kass, R. E., Raftery, A. E., and Wasserman, L. (1997), "Computing Bayes Factors by Combining Simulation and Asymptotic Approximations," *Journal of the American Statistical Association*, 92, 903–915.

Diggle, P. J. (1983), *Statistical Analysis of Spatial Point Patterns*, London: Academic Press.

Fraley, C., and Raftery, A. E. (1998), "How Many Clusters? Which Clustering Method? Answers via Model-Based Cluster Analysis," *Computer Journal*, 41, 578–588.

Gelman, A., and Rubin, D. B. (1992), "Inference From Iterative Simulation Using Multiple Sequences (With Discussion)," *Statistical Science*, 7, 457–511.

Gilks, W. R., Richardson, S., and Spiegelhalter, D. J. (eds.) (1996), *Markov Chain Monte Carlo in Practice*, London: Chapman & Hall.

Hastings, W. K. (1970), "Monte Carlo Sampling Methods Using Markov Chains and Their Applications," *Biometrika*, 57, 97–109.

Holmes, Q. A., Schwartz, C. R., Seldin, J. H., Wright, J. A., and Witter, L. J. (1995), "Adaptive Multispectral CFAR Detection of Land Mines," in *Detection and Technologies for Mines and Minelike Targets*, Volume 2496 of *Proceedings of SPIE*, eds. A. C. Dubey, I. Cindrich, J. M. Ralston, and K. Rigano, pp. 421–432.

Hough, P. V. C. (1962), "Method and Means for Recognizing Complex Patterns," U.S. Patent 3,069,654.

Kass, R. E., and Raftery, A. E. (1995), "Bayes Factors," *Journal of the American Statistical Association*, 90, 773–795.

Lake, D. E., and Keenan, D. M. (1995), "Identifying Minefields in Clutter via Collinearity and Regularity Detection," in *Detection and Remediation Technologies for Mines and Minelike Targets*, Volume 2496 of *Proceedings of SPIE*, eds. A. C. Dubey, I. Cindrich, J. M. Ralston, and K. Rigano, pp. 519–530.

Lake, D. E., Sadler, B., and Casey, S. (1997), "Detecting Regularity in Minefields Using Collinearity and a Modified Euclidean Algorithm," in *Detection and Remediation Technologies for Mines and Minelike Targets II*, Volume 3079 of *Proceedings of SPIE*, eds. A. C. Dubey and R. Barnard, pp. 508–518.

Muise, R. R., and Smith, C. M. (1992), "Nonparametric Minefield Detection and Localization," Technical Report CSS-TM-591-91, Naval Surface Warfare Center, Coastal Systems Station.

——— (1995), "A Linear Density Algorithm for Patterned Minefield Detection," in *Detection and Remediation Technologies for Mines and Minelike Targets*, Volume 2496 of *Proceedings of SPIE*, eds. A. C. Dubey, and I. Cindrich, J. M. Ralston, and K. Rigano, pp. 586–593.

Raftery, A. E. (1996), "Hypothesis Testing and Model Selection," in *Markov Chain Monte Carlo in Practice*, eds. W. R. Gilks, S. Richardson, and D. J. Spiegelhalter, London: Chapman & Hall, pp. 163–188.

Raftery, A. E., and Lewis, S. M. (1992), "How Many Iterations in the Gibbs Sampler?" in *Bayesian Statistics 4*, eds. J. M. Bernardo, J. O. Berger, A. P. Dawid, and A. F. M. Smith, Oxford: Oxford University Press, pp. 765–766.

——— (1996), "Implementing MCMC," in *Markov Chain Monte Carlo in Practice*, eds. W. R. Gilks, S. Richardson, and D. J. Spiegelhalter, London: Chapman & Hall, pp. 115–130.

Stanford, D. C., and Raftery, A. E. (2000), "Finding Curvilinear Features in Spatial Point Patterns: Principal Curve Clustering With Noise," *IEEE Transactions on Pattern Analysis and Machine Intelligence*, 22, 601–609.

Witherspoon, N. H., Holloway Jr., J. H., Davis, K. S., Miller, R. W., and Dubey, A. C. (1995), "The Coastal Battlefield Reconnaissance and Analysis (COBRA) Program for Minefield Detection," in *Detection and Remediation Technologies for Mines and Minelike Targets, Proceedings of SPIE*, eds. A. C. Dubey, I. Cindrich, J. M. Ralston, and K. Rigano, pp. 500–508.